frontiers in Energy Research

ORIGINAL RESEARCH
published: 18 March 2022
doi: 10.3389/fenrg.2022.816246

Risk Assessment of AC/DC Hybrid Distribution Network considering New Energy and Electric Vehicle Access

Jie Dong[1], Jianjun Zhao[1], Ziyue Liu[2], Yang Li[1], Zhongshu Yu[2], Jialin Liu[1] and Zhenhao Wang[2]*

[1]Smart Distribution Network Center, State Grid Jibei Electric Power Co., Ltd., Qinhuangdao, China, [2]Key Laboratory of Modern Power System Simulation and Control & Renewable Energy Technology, Ministry of Education (Northeast Electric Power University), Jilin, China

In view of the operational risk issues such as safety and economy caused by the connection of new energy and multiple types of electric vehicles (EVs) to the AC–DC distribution network, an AC–DC distribution network operational risk assessment method that takes into account multiple risk factors is proposed. First, a probability distribution model of scenery output and EV timing is constructed, and the starting charge state of multiple types of EVs is replaced by the number of daily driving miles subjectively set; then, based on the complex network theory, timing safety indicators, such as voltage overrun risk and branch power overload operation risk, are proposed, and the economic risk is established according to the economic operation of the distribution grid; Furthermore, a risk assessment matrix for grid-connected EVs with different capacities is constructed, and the principal component analysis (PCA) method is used to reduce the dimension of the risk assessment matrix and calculate the objective weight coefficient; finally, taking the improved IEEE 33 node AC/DC power distribution system as an example, the comprehensive risk evaluation based on PCA is compared with the traditional one, and the results show that when the safety and economic risk factors are considered at the same time, the operation risk in a certain range has a downward trend when the proposed method is adopted, which has a positive guiding significance for the planning of EV capacity in a certain area.

Keywords: electric vehicle, risk assessment index, complex network, AC/DC distribution networks, new energy

Edited by:
Mohd Hasan Ali,
University of Memphis, United States

Reviewed by:
Mehdi Firouzi,
Islamic Azad University, Abhar, Iran
Katarzyna Pietrucha-Urbanik,
Rzeszów University of Technology, Poland

****Correspondence:***
Ziyue Liu
1055435004@qq.com

Specialty section:
This article was submitted to Smart Grids, a section of the journal Frontiers in Energy Research

Received: *16 November 2021*
Accepted: *24 February 2022*
Published: *18 March 2022*

Citation:
Dong J, Zhao J, Liu Z, Li Y, Yu Z, Liu J and Wang Z (2022) Risk Assessment of AC/DC Hybrid Distribution Network considering New Energy and Electric Vehicle Access. Front. Energy Res. 10:816246. doi: 10.3389/fenrg.2022.816246

INTRODUCTION

In recent years, with the rapid increase of new energy and electric vehicle (EV) access capacity, the structure, flow, and operation mode of the AC and DC distribution network have undergone tremendous changes (Liang et al., 2020). On the one hand, the output of DG (distributed generation) has randomness and uncertainty, which will cause negative effects such as line overload, reduced power quality, and increased system loss (Yang et al., 2020a); on the other hand, the random charging behavior of EVs will provide a safe and economically stable operation of the power system bringing new risks and challenges (Chen et al., 2019). Therefore, evaluating the operational risks of DG and EV after being connected to the power grid is an urgent problem to be solved in the power system.

The risk assessment for the simultaneous access of DG and EVs to the AC/DC distribution network is mainly divided into two aspects: risk assessment method and risk assessment index construction. The traditional risk assessment analysis method mainly follows the reliability assessment method, which can usually be divided into the analytical and simulation methods (Lu and Yuan, 2017). Nan et al., (2020) established a risk assessment system from four levels for EV fast charging stations using the AHP (analytic hierarchy process) and entropy weight methods to determine the weight of each level of the index and finally combined with the fuzzy comprehensive evaluation method to quantify the evaluation results; Xiong et al., (2016), based on the stochastic power flow of the full probability theory, established and solved the level 2 risk index, established the comprehensive risk assessment index, and realized the quantitative assessment of the risk of the distribution network; Hu et al., (2016) established the dynamic distribution model of EV charging power using the semi-invariant probabilistic power flow algorithm and solved the risk indicators of node voltage and branch power flow over-limit so as to analyze the security risk of the electric power distribution network. Although the abovementioned studies have made certain contributions to risk assessment methods, most of them rely on expert evaluation (Yuan et al., 2016) or semi-quantitative analysis when determining indicator weights. They are susceptible to subjective factors and are often not comprehensive enough to consider the true size of risk indicators.

In terms of the construction of the risk index system, the index system that uses the degree of severe loss to describe the consequences of operating events has developed more maturely. Liu et al., (2015) defined the calculation expressions of risk indicators such as voltage overruns, probability of line fluctuations, and severity of accidents and conducted a comprehensive risk assessment of the power grid and quantified the differences of components; Zhang et al., (2019) fully considered wind power, and based on the uncertainty of EV access to the distribution network, the load aggregator response reliability and risk cost indicators are proposed based on fuzzy theory. In addition, harmonic risk (Zhao et al., 2014), load reduction risk (Wang et al., 2018), flexibility risk (Li et al., 2015) and other risk indicators are also involved in research, but most of them are limited to a single risk indicator that considers safety or economy and does not consider operational risks. Due to variable factors and dynamic processes, it is impossible to clearly grasp the operating status of the power system.

At the same time, the abovementioned documents are all researched under the premise of considering a single type of EV, and the charging power remains unchanged. Yang et al., (2020b) built a weighted basis for the scenario where DG and three types of variable power EV charging loads are simultaneously connected to the distribution network, entropy voltage, and power flow limit risk, but it did not further analyze the EV type and charging mode and failed to objectively consider the operation risk status of the distribution network from multiple factors. Therefore, it is necessary to establish a set of multilevel risk indicator system and objective and reasonable comprehensive evaluation methods, thereby reducing repeated risk information and better analyzing the operating status. This study analyzes the stochastic characteristics of DG output and EV charging load and constructs a time-series model of constant current–constant voltage (CC–CV) variable power multitype EV charging load based on daily driving mileage; proposes a short-term safety risk index based on the complex network theory, while introducing an economic risk that includes the operating profit; a three-dimensional and multi-angle risk index system is established; and the principal component analysis (PCA) method is used to comprehensively evaluate the operation risk of the distribution network under different EV capacities. The validity of the proposed risk index and the rationality of the comprehensive evaluation method are verified by numerical example analysis. The results show that the proposed method can actively guide the safe, economical, and stable operation of DG and EV in the distribution network.

WIND POWER, PHOTOVOLTAIC, AND CONVENTIONAL LOAD MODELS

Wind Power Model

Wind power output is mainly determined by wind speed, and the statistical characteristics of wind speed obey the two-parameter Weibull distribution (Liu et al., 2017). Therefore, the expression of the distribution function of the active power output P_w of the wind turbine is as follows:

$$F(P_\mathrm{w}) = \begin{cases} 0 & 0 \le v < v_\mathrm{ci},\ v \ge v_\mathrm{co} \\ 1 - \exp\left\{ - \left[\left(1 + \dfrac{v_\mathrm{cr} - v_\mathrm{ci}}{v_\mathrm{ci} P_\mathrm{r}} P_\mathrm{w} \right) \dfrac{v_\mathrm{ci}}{c_\mathrm{w}} \right]^{k_\mathrm{w}} \right\} + , \\ \exp\left[- (v_\mathrm{co}/c_\mathrm{w})^{k_\mathrm{w}} \right] & v_\mathrm{ci} \le v < v_\mathrm{cr} \end{cases} \tag{1}$$

where P_r is the rated output power of the fan; v is the wind space; v_co, v_ci, and v_cr are cut-out, cut-in, and rated wind speed, respectively; and k_w and c_w are scale and shape parameters, respectively.

Photovoltaic Power Generation Model

The intensity of solar light varies with the geographical environment and location. Based on a large amount of measurement data, beta distribution (Zhang et al., 2013) can be used to represent the distribution of solar light intensity in a day. Then, the probability density function of photovoltaic power generation's active power output is as follows:

$$f(P_\mathrm{solar}) = \frac{\Gamma(\alpha+\beta)}{\Gamma(\alpha)\Gamma(\beta)} \left(\frac{P_\mathrm{solar}}{P_\mathrm{solar,\,max}} \right)^{\alpha-1} \left(1 - \frac{P_\mathrm{solar}}{P_\mathrm{solar,\,max}} \right)^{\beta-1}, \tag{2}$$

$$\begin{cases} \Gamma(g) = \int_0^\infty \mathrm{x}^{\mathrm{g}-1} \mathrm{e}^{-\mathrm{x}} \mathrm{dx} \\ P_\mathrm{solar} = rA\eta \end{cases}, \tag{3}$$

where $\Gamma(\cdot)$ is the gamma function; α and β are two parameters that characterize the shape of the beta distribution function; P_solar and $P_\mathrm{solar,max}$ are the actual output and maximum output of the photovoltaic array, respectively; r is solar irradiance; and η and A are the power conversion efficiency and the total area of the photovoltaic array, respectively.

TABLE 1 | Parameters of the constant current-constant voltage two-stage variable power charging process of the lithium battery.

E_0	K_0	A	B	R
1.0834 U_n	0.05645 U_n/C_0	0.08496	60.0619/C_0	0.01 U_n/C_0

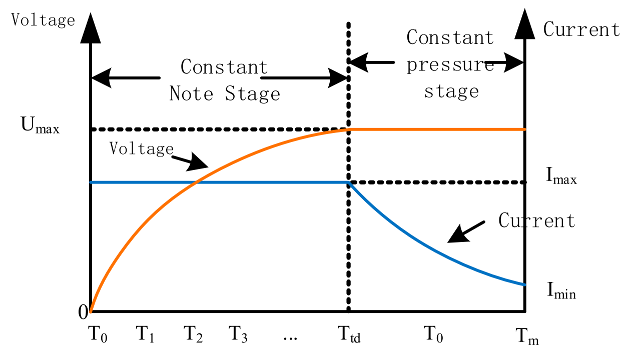

FIGURE 1 | Current and voltage changes in the CC–CV charging mode.

Conventional Load Model

The conventional load at any time adopts normal distribution to reflect its randomness and uncertainty. The probability density function of the conventional load active power P_{LD} and active power Q_{LD} is as follows:

$$\begin{cases} f(P_{\mathrm{LD}}) = \dfrac{1}{\sqrt{2\pi}\lambda_{\mathrm{LP},t}\mu_{\mathrm{LP},t}} \exp\left(-\dfrac{P_{\mathrm{LD}}-\mu_{\mathrm{LP},t}}{2\lambda_{\mathrm{LP},t}^2\mu_{\mathrm{LP},t}^2}\right) \\ f(Q_{\mathrm{LD}}) = \dfrac{1}{\sqrt{2\pi}\lambda_{\mathrm{LQ},t}\mu_{\mathrm{LQ},t}} \exp\left(-\dfrac{Q_{\mathrm{LD}}-\mu_{\mathrm{LQ},t}}{2\lambda_{\mathrm{LQ},t}^2\mu_{\mathrm{LQ},t}^2}\right) \end{cases}, \quad (4)$$

where $\mu_{\mathrm{LP},t}$ and $\mu_{\mathrm{LQ},t}$ are the expected values of the active power and reactive power of the conventional load at time, respectively; and $\lambda_{\mathrm{LP},t}$ and $\lambda_{\mathrm{LQ},t}$ are the coefficients of variation of the active power and reactive power of the conventional load at time t, respectively.

ELECTRIC VEHICLE PROBABILITY DISTRIBUTION MODEL

The factors that affect EV charging load can be summarized as charging characteristics, charging period, and charging mode. The following three influencing factors will be analyzed separately to establish a mathematical probability distribution model.

Electric Vehicle Charging Characteristic Model

The EV charging process meets the charging characteristics of lithium batteries. It is a CC–CV variable power charging method. When the battery state of charge is low and the battery internal resistance is relatively stable, the constant current method is used for fast charging. As the charging time increases, the charging voltage increases after reaching $U_{\max}$, the equivalent internal resistance of the battery increases rapidly, entering the constant voltage charging stage, the charging current decays exponentially, and the constant voltage charging process accounts for less than 1% of the constant current charging process. In order to simplify the calculation, this study analyzes only the constant current charging process. The charging process parameters are shown in **Table 1**. The voltage and current variation curves during EV charging are shown in **Figure 1**, and the specific formulas are shown in literature (Zheng et al., 2012). The charging process parameters are shown in **Table 1**.

TABLE 2 | Parameter setting of the electric vehicle's battery.

EV type	Private car	Bus	Taxi	Official car
Battery capacity/(A·h)	200	600	200	200
Rated charging current/A	20/150	100/200	150	20
Battery voltage rating/V	316.8	540	316.8	316.8
End voltage maximum/V	345	597	359	345
Maximum mileage/km	400	250	400	400
Charging efficiency/%	90	90	90	90

Therefore, the charging power of the jth EV can be defined as $P_{car,j}$, and the specific parameters are shown in **Table 2**.

$$P_{\mathrm{car},j} = U_{\mathrm{batt}} i_{\mathrm{car}}, \quad (5)$$

where U_{batt} is the terminal voltage of the lithium battery; i_{car} is the EV charging current.

Electric Vehicle Charging Period Model

The initial charging time, daily mileage, and EV charging period are very closely related, so this study is based on the 2017 and 2018 National Family Travel Survey (NHTS) data published by the US Federal Highway Administration on the entire network (Guo et al., 2020; U.S. Department of Transportation, 2018); the Monte Carlo simulation (MCS) method is used to fit the normal distribution of EV daily mileage, as shown in **Eq. 6**.

$$f(d) = \frac{1}{\sqrt{2\pi} d\sigma_d} \exp\left(-\frac{\ln d - \mu_d}{2\sigma_d^2}\right), \quad (6)$$

where μ_d and σ_d are the expected value and standard deviation of the normal distribution function, respectively, and different values are selected according to the user's driving behavior.

The initial charging time of EV satisfies the normal distribution shown in **Eq. 7**.

$$f(t) = \frac{1}{\sqrt{2\pi}\sigma_t} \exp\left[-\frac{(t-\mu_t)^2}{2\sigma_t^2}\right], \quad (7)$$

where μ_t and σ_t are the expected value and standard deviation of the normal distribution function, respectively, and different values are selected according to the user's driving behavior.

TABLE 3 | Driving characteristic parameters of the EV.

EV types	Charging periods	Probability distribution of starting charging moments	Probability distribution of daily miles travelled
Bus	10:00–16:30, 23:00 to 05:30 next day	N(14,1^2), N(23,1^2)	N(4.4,0.35^2)
Taxi	02:00–05:00, 11:30–14:30	N(4,1^2), N(13,1^2)	N(5.1,0.35^2)
Private car	09:00–12:00, 14:00–17:00, 19:00 to 07:00 next day	N(9,1^2), N(14,2^2), N(19,2^2)	N(3.58,0.88^2)
Official car	19:00 to 07:00 next day	N(19,2^2)	N(3.58,0.89^2)

The charging time T is calculated according to the daily mileage d, as shown in formula **Eq. 8**.

$$T = \frac{dW_{100}}{100P_{\mathrm{car},j}\eta_{\mathrm{car}}}, \tag{8}$$

where W_{100} is the power consumption of EV driving 100 km; η_{car} is the charging efficiency of the EV.

Electric Vehicle Charging Mode Analysis

The charging mode has a great influence on the EV charging power. At present, the main charging modes of EVs include slow charging, regular charging, and fast charging. Generally, different charging modes are distinguished by a given constant current. In the following paragraphs, according to the driving characteristics of different types of EVs, the charging mode that meets the actual situation is selected.

The driving range of a fully charged private car battery is much greater than the average daily driving range, so one charging cycle a day can meet the daily driving demand of a private car. Private cars can be charged in the parking lot of the workplace from 09:00–12:00 and 14:00–17:00 or charged in the parking lot of residential areas from 19:00 to 07:00 the next day, charging in three periods. The probabilities are 20, 10, and 70%. If charging in the parking lot of the work unit, the charging time does not exceed 3 h; then, the fast charging mode is chosen with larger constant current; if charging in the parking lot of a residential area, the charging can continue all night; then, the regular constant current moderate charging mode is chosen. Official vehicles are mainly used for daily official travel of government agencies. Long-distance travel is not considered. Its driving characteristics are similar to private cars. It can meet the charging demand even if it is charged once a day. The charging period is from 19:00 to 07:00 the next day. The constant current moderate regular charging mode is chosen.

It is difficult to meet the operational requirements of actual work for buses and taxis to be charged only once a day. Generally, two charging cycles a day are adopted. The bus operating time is 06:00–22:00 and the route is relatively fixed. It can be charged centrally. Charging is not arranged during the peak operation period during the day. During the 10:00–16:30 shift and lunch break, the bus will be charged with a constant current. Charging in the charging mode and in the regular charging mode with moderate current from 23:00 to 05:30 is conducted the next day. Taxis have limited rest time and need to replenish electricity in time. Therefore, taxis are charged in a constant-current fast charging mode during the two periods of 02:00–05:00 and 11:30–14:30.

The specific parameters of the four EVs are set according to the influence of the different charging modes on the magnitude of the charging power **Table 3**.

ESTABLISHMENT OF ELECTRIC VEHICLE CHARGING RISK INDICATORS

Short-Term Security Risk Indicators

Severity of Loss Based on Complex Network Theory

As a complex system, each node of the power grid does not exist independently but as a whole that restricts and influences each other. The vulnerability of each component is not only related to its structural position in the power grid but also to other components when the power grid is running. The influence of the node is related. Therefore, when evaluating the risk of DG and EV connecting to the AC/DC distribution network, it is necessary to comprehensively consider the impact of various factors. Therefore, this study proposes a short-term security risk assessment model for power grids that combines network structure vulnerability and risk theory. The importance of the node comprehensively considers the degree of the node, the betweenness (Shi et al., 2018), and the proportion of the conventional load connected to the node. The importance of the branch is measured by the degree and betweenness of the line, and the calculation formulas are as follows:

$$\rho_{\mathrm{v,i}} = \alpha_1 D_{\mathrm{v,i}} + \alpha_2 B_{\mathrm{v,i}} + \alpha_3 N_{\mathrm{Pi}}, \tag{9}$$

$$\rho_{1,l} = \beta_1 D_{1,l} + \beta_2 B_{1,l}, \tag{10}$$

where $\rho_{\mathrm{v},i}$ and $\rho_{\mathrm{l},l}$ are the node importance of the node and the branch importance of the line, respectively; $D_{\mathrm{v},i}$ and $B_{\mathrm{v},i}$ are the degree and betweenness of the node, respectively; $N_{\mathrm{P}i}$ is the power injected into the node; $D_{\mathrm{l},l}$ and $B_{\mathrm{l},l}$ are the degree and betweenness of the line, respectively; α_1, α_2, and α_3 are the weight coefficients of node degree, node betweenness, and node injection power, respectively, and $\alpha_1 + \alpha_2 + \alpha_3 = 1$; β_1 and β_2 are the weight coefficients of the line degree and line betweenness, respectively; and $\beta_1 + \beta_2 = 1$. In this study, the AHP method is used to determine the size of each weight coefficient.

Short-Term Security Risk Indicators

EV charging load will bring short-term security risks to the power grid. Impact indicators include node voltage over-limit risk indicators and line power over-limit risk indicators. The specific calculation method is as follows.

a) The calculation formula of the node voltage over-limit operation risk index is.

$$R_{\mathrm{v,i}}(t) = \sum_{j=1}^{n_{\mathrm{v,i}}(t)} \rho_{\mathrm{v,i}} S_{\mathrm{v,j}}(t) p\left(S_{\mathrm{v,j}}\right), \tag{11}$$

$$S_{v,j}(t) = \begin{cases} V - V_{\max} & V > V_{\max} \\ 0 & V_{\min} \le V \le V_{\max} \\ V_{\min} - V & V < V_{\min} \end{cases}, \tag{12}$$

where $R_{v,i}(t)$ is the value of the risk index value of the voltage over-limit operation of the node at time t; $n_{v,i}(t)$ is the number of voltage states of node i at time t, where the number of voltage states is the number of times the voltage per unit value of the probability flow node i crosses the upper and lower limits; $p(S_{v,j})$ is the probability of the jth voltage state; $S_{v,j}(t)$ is the voltage loss severity of the jth voltage state of node i at time t; and V, $V_{\max}$, and $V_{\min}$ are the voltage qualified value and the unit value of the upper and lower limits, respectively.

b) The calculation formula of the risk index of line power exceeding the limit is.

$$R_{1,l}(t) = \sum_{k=1}^{n_{1,l}(t)} \rho_{1,l} S_{1,k}(t) p(S_{1,k}), \tag{13}$$

$$S_{1,k}(t) = \begin{cases} L_l - 0.9 & L_l > 0.9 \\ 0 & L_l \le 0.9 \end{cases}, \tag{14}$$

where $R_{l,l}(t)$ is the power limit risk index value of line l at time t; $n_{l,l}(t)$ is the number of power flow states of line l at time t, where the number of power flow states is the number of times that the active power flow of branch l of the probability power flow exceeds the limit; $p(S_{l,k})$ is the probability of the kth power flow state; $p(S_{l,k})$ is the severity of the active power flow loss of the branch in the kth power flow state of line l at time t; and L_l is the ratio of actual active power to rated active power of line l.

In this study, $R_{l,l}(t)$ is used to characterize the short-term comprehensive safety risk coefficient of system operation, $R_{sys}^{v}(t)$ is used to characterize the voltage risk caused by the over-limit of the node voltage of the AC/DC distribution network system and its distribution uncertainty, and $R_{sys}^{l}(t)$ is used to characterize the over-limit of the branch power of the AC/DC distribution network system and its distribution uncertainty. The tidal current risks caused are as follows:

$$R_{\mathrm{SRI}} = \gamma_1 R_{\mathrm{sys}}^{v}(t) + \gamma_2 R_{\mathrm{sys}}^{1}(t), \tag{15}$$

where γ_1 and γ_2 are the security risk weight coefficient, and $\gamma_1 + \gamma_2 = 1$。

Economic Risk Indicators

The ERI (economic risk indicator) of DG and EV charging loads connected to the AC/DC distribution network comprises two parts: ELLR (economic line-loss risk) and EPLR (economic operational profit or loss risk). The formula is as follows:

$$C^{\mathrm{ERI}}(t) = C^{\mathrm{ELLR}}(t) - C^{\mathrm{EPLR}}(t), \tag{16}$$

$$C^{\mathrm{ELLR}}(t) = C^{\mathrm{price}}(t) P^{\mathrm{loss}}(t), \tag{17}$$

$$C^{\mathrm{EPLR}}(t) = \sum_{i'=1}^{n} C_{i'}^{\mathrm{sell}}(t) + C^{\mathrm{env}}(t) - \sum_{i'=1}^{n} C_{i'}^{\cos t}(t), \tag{18}$$

$$C_{i'}^{\mathrm{sell}}(t) = S_{i'}^{\mathrm{DG}}(t) P_{i'}^{\mathrm{DG}}(t), \tag{19}$$

$$C_{i'}^{\mathrm{cost}}(t) = \sum_{m=1}^{N} \sum_{i'=1}^{n} \mu_{i'} P_{i',m}^{\mathrm{DG}}(t), \tag{20}$$

$$C^{\mathrm{env}}(t) = \sum_{j=1}^{m'} M_j C_j \left(P^{\mathrm{WODG}}(t) - P^{\mathrm{WDG}}(t)\right), \tag{21}$$

where $C^{ERI}(t)$ is the ERI value of the AC/DC distribution network at time t; $C^{ELLR}(t)$ and $C^{EPLR}(t)$ are, respectively, the ELLR and EPLR index values of the AC/DC distribution network at time t; $C^{price}(t)$ is the electricity price of the AC/DC distribution network at time t; $P^{loss}(t)$ is the power loss of the AC/DC distribution network at time t; $C^{env}(t)$ is the government subsidy income from the AC/DC distribution network at time t; $C_{i'}^{\cos t}(t)$ and $C_{i'}^{sell}(t)$ are, respectively the operation and maintenance cost and electricity sales revenue of the i'-th DG at time t; n is the number of DG; $S_{i'}^{DG}(t)$ is the time-varying electricity price per unit power of the i'-th DG at time t; $P_{i'}^{DG}(t)$ is the active output power of the i'-th DG at time t; N is the number of types of DG; $\mu_{i'}$ is the maintenance cost per unit power of the i'-th DG; $P_{i',m}^{DG}(t)$ is the active output power of the i'-th DG of the mth type at time t; $P^{WDG}(t)$ and $P^{WODG}(t)$ are the power obtained by the AC/DC distribution network from the large power grid before and after the DG is connected at the time t, respectively; M_j is the emission coefficient of category jth pollutant gas per unit power generation of the AC/DC distribution network; C_j is the treatment cost of the jth polluted gas; and m' is the number of polluted gas categories.

PRINCIPAL COMPONENT ANALYSIS–BASED COMPREHENSIVE RISK ANALYSIS

In order to fully consider the uncertainty of EV charging time and charging location and its impact on the power distribution system, EV capacity (Yang et al., 2020b) is defined as the sum of the rated charging power of all EVs in the charging and non-charging states in an area. According to the risk indicators mentioned above, in order to ensure the safe and stable operation of DG and EV in the distribution network, the PCA method (Xiao et al., 2018) is used to analyze the risks caused by different EV capacities to the distribution network, and a small number of risk variables are used to replace the original large number of risk variables and can contain the full content of the original input risk variable. P risk indicators $x_1, x_1, \cdots, x_p$are defined, whose weights are $c_1, c_2, \cdots c_p$, respectively; then, the weighted sum of the risk indexes is $s = c_1 x_1 + c_2 x_2 + \cdots + c_p x_p$. When the power grid is connected to different EV capacities, there is a corresponding comprehensive evaluation result, and the comprehensive evaluation result when h different EV capacities

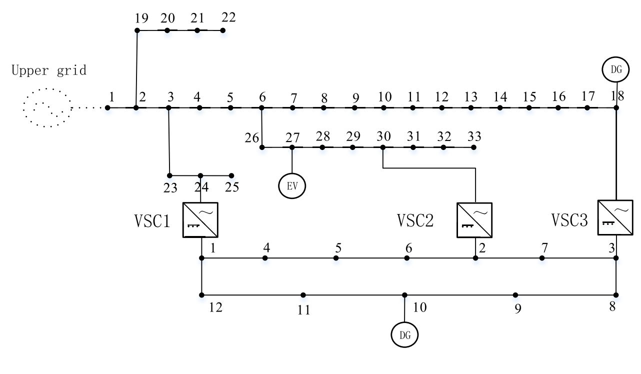

FIGURE 2 | Improved 33-node AC/DC system.

are connected is recorded as $s_1, s_2, \cdots, s_h$. The specific steps of the PCA method are as follows. 1) The calculated risk index data are standardized, its dimension is eliminated, and a standardized risk index matrix $\boldsymbol{B} = [b_{i''}(m'')]_{h\times k} = [\boldsymbol{B}_1, \boldsymbol{B}_2, \cdots, \boldsymbol{B}_k]$is obtained, whose elements are shown in formula **Eq. 22**.

$$b_{i''}\left(m''\right) = \left(x_{i''}\left(m''\right) - \bar{x}_{i''}\right) \Big/ s_{i''}. \tag{22}$$

Among them, $\bar{x}_{i''} = \sum_{m=1}^{h} x_{i''}(m'')/h$ is the indicator mean; $s_{i''} = \sqrt{\sum_{m''=1}^{h} (x_{i''}(m'') - \bar{x}_{i''})^2/h}$ is the indicator standard deviation. After normalization, matrix **B** satisfies $E(B_{i''}) = 0$ and $D(B_{i''}) = 1\,(i'' = 1, 2, \ldots, k)$.

According to the standardized risk index matrix **B**, the correlation coefficient matrix **R** is calculated after processing by the Z-Score method. Since the correlation coefficient matrix is equal to the covariance matrix, and **R** is a positive definite matrix, the eigenvalue $\lambda_1 \geq \lambda_1 \geq \cdots \geq \lambda_{m''} \geq 0$ of **R**is calculated and the corresponding characteristics vector $u_1, u_2, \cdots, u_{m''}$; then, the calculation expression of the ith principal component $Y_{i'''}\,(i''' = 1, 2, \cdots, p)$ is as follows:

$$\boldsymbol{Y}_{i'''} = \boldsymbol{B}_{i'''}^{T} \boldsymbol{u}_{i'''}. \tag{23}$$

The proportion of the variance of the i''' principal component $\mathbf{Y}_{i'''}$ in the total variance is defined as the contribution rate $\nu_{i'''}$, which is used to reflect the comprehensive ability of the original p indicators. The cumulative contribution rate γ is defined as the total comprehensive ability of the first k principal components. The formulas for $\nu_{i'''}$ and γ are as follows:

$$\nu_{i'''} = \lambda_{i'''} \Big/ \sum_{i'''=1}^{p} \lambda_{i'''}. \tag{24}$$

$$\gamma = \sum_{i'''=1}^{k} \lambda_{i'''} \Big/ \sum_{j'=1}^{p} \lambda_{j'}. \tag{25}$$

If the cumulative variance of the principal components reaches a certain proportion, the original index can be replaced by the corresponding principal component, and the comprehensive risk assessment index result can be calculated by the linear superposition of the abovementioned principal components, namely:

TABLE 4 | EVC proportion of various types of electric vehicles.

EV types	Private car	Bus	Taxi	Official car
EVC(%)	54	18	18	10

$$F = \nu_1 Y_1 + \nu_2 Y_2 + \cdots + \nu_{m''} Y_{m''}. \tag{26}$$

On the premise of retaining the main information of the original data, PCA effectively reduces the correlation between the evaluation indicators and the data dimension, so the obtained evaluation is more credible. At the same time, since the comprehensive risk assessment takes the contribution rate of each principal component as the weight, it not only avoids the drawbacks of subjective weighting but also fully reflects the information value contained in the risk index.

CASE ANALYSIS

Simulation of Distributed Generation Output and Electric Vehicle Charging Load in the AC/DC Distribution Network

In this study, the improved IEEE 33 node distribution system is selected as a simulation example. The system is a 10 kV network with a reference voltage of 12.66 kV and a three-phase power reference value of 10 MV A. Its improved topology is shown in **Figure 2** with node 1 as a balancing node and the voltage set to 1.05 p. u. The wind power is equivalently connected to node 18, the PV is equivalently connected to node 33, and the EV charging load of 13 MW is equivalently connected at node 8, with a total expected peak value of 3.715 MW for the conventional load. The relevant parameters of the EV are shown in **Tables 1–4**.

The simulation parameters and distribution parameter variation curves of the DG are shown in **Table 5** and **Figure 3**, respectively, and the DG output curve is shown in Appendix **Figure 4**.

The DG tariff setting reference (Ju et al., 2019). The power factor of both the load and the power source is 0.95. The O &M cost of both wind and PV is \$55. The calculation process for distribution network operational risk is shown in **Figure 5**.

In this study, the AHP method is used to determine the weight coefficients of the risk indicators in **Section 3.1**, which can be obtained as $\alpha_1 = 0.2$, $\alpha_2 = 0.2$, $\alpha_3 = 0.6$, $\beta_1 = 0.5$, $\beta_2 = 0.5$, $\gamma_1 = 0.5$, and $\gamma_2 = 0.5$. MCS accuracy k_e is set to 0.05%. In order to make the maximum variance coefficient of voltage, branch power flow, and network loss (Zhao et al., 2009; Li et al., 2021), $d_{v,\max}$, $d_{l,\max}$, and d_{loss} are all less than k_e, and the number of simulations is set to 5,000.

According to the model in **Section 2** and **3**, the expected charging power values of 4 EV types are obtained based on the MCS method, as shown in **Figure 5**. It can be seen from **Figure 6** that for private cars, they are charged in a relatively large constant current fast charging mode between 09:00–12:00 and 14:00–17:00, resulting in a double-peak load state; at 00: 00: during 00–07:00 and 19:00–24:00, although the conventional charging mode is

TABLE 5 | Simulation parameters of wind power and photovoltaic power.

Cut-in wind speed v_{ci}	Rated wind speed v_{cr}	Cut-out wind speed v_{co}	Fan rated power (MW) P_w	Total photovoltaic cell area (m) A	Electrical energy conversion efficiency (%) η	Maximum PV intensity r_{max}
3 m/s	13 m/s	25 m/s	2	$14{,}00^2$	14	1.133 kW/m^2

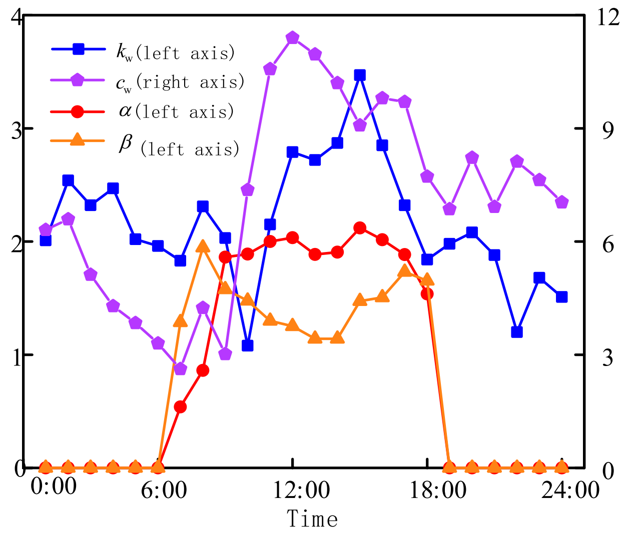

FIGURE 3 | Photovoltaic power distribution parameters α and β and wind speed distribution parameters c_w and k_w.

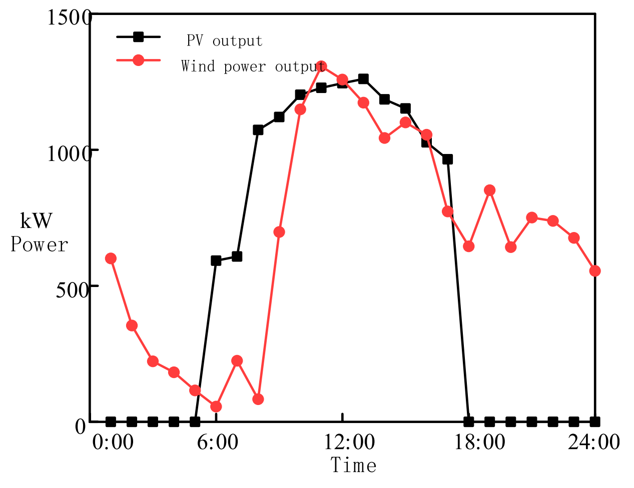

FIGURE 4 | Output of wind-PV in each period.

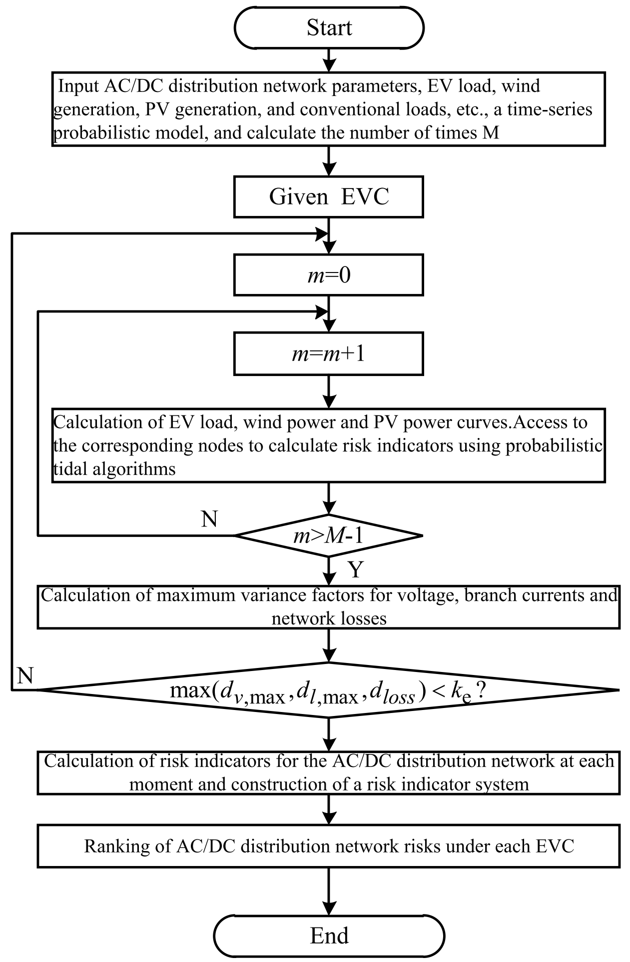

FIGURE 5 | Calculation process of distribution network operation risk.

adopted, a large number of private car access also caused load peaks. Among them, the private car charging load and regular load during 19:00–24:00 both reached the peak value, which intensified the operation risk of the power grid. During the period of 00:00–07:00, the battery power of most private cars was close to saturation, which caused the charging load of private cars to drop. For official vehicles, the regular charging mode is adopted during the period from 19:00 to 24:00, forming a single peak load, which aggravates the total load during this period to a certain extent. For buses, the fast charging mode is adopted during the period of 13:00–16:00 so that the load reaches the peak during the day; the regular charging is adopted during the period of 00:00–01:00 and 23:00–24:00 The mode makes the night load increase, which has an impact on the operation risk of the distribution network, but it complements other types of EV charging loads, which reduces the load peak-to-valley difference to a certain extent. For taxis, the fast charging mode with a relatively large constant current is adopted during the period of 03:00–05:00, which dominates the EV charging load; the fast charging mode is also adopted during the period of 12:00–14:00.

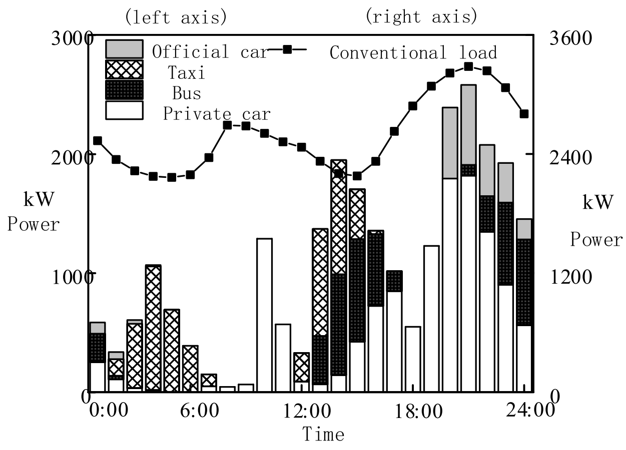

FIGURE 6 | Expected charging power for four EV types.

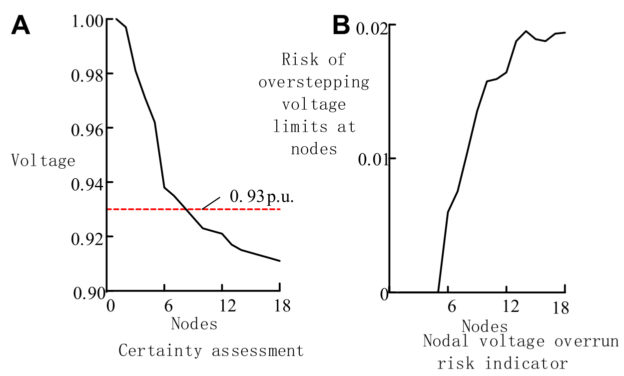

FIGURE 7 | Results of deterministic assessment and proposed short-term safety risk indicator: **(A)** Certainty assessment. **(B)** Nodal voltage overrun risk indicator.

This intensified the peak of the daytime charging load but reduced the volatility of the load to a certain extent. In summary, it can be seen that the charging load fluctuates sharply within a day, so it is necessary to analyze the risk of power grid operation.

Risk Analysis of Safe and Economic Operation of Distributed Generation and Electric Vehicle Connected to the AC/DC Distribution Network

Analysis of Short-Term Security Risk Indicators

In order to study the rationality and necessity of the short-term safety risk indicator, this study first compares the deterministic assessment and the short-term safety risk indicator proposed in this study, that is, an equivalent EV charging load of 13 MW is connected at node 8, and the AC voltage at nodes 1–18 is assessed during the period 20:00–21:00; the results are shown in **Figure 7** (AC voltages in the figure are the standardized values). The stochastic nature of the DG output power, EV charging power, and conventional load is ignored in the deterministic assessment. The average equivalent access node power was used to calculate the AC node voltage. As can be seen from **Figure 7A**, when the

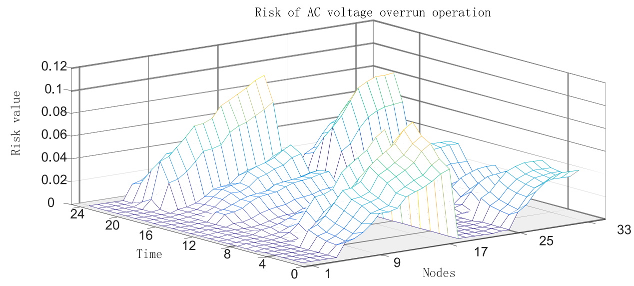

FIGURE 8 | Risk of over-voltage operation of AC distribution network nodes.

deterministic assessment is taken, nodes 9–18 are the nodes with voltages exceeding 0.93 p. u. In other words, only 10 nodes have voltage overruns under the deterministic assessment; however, as can be seen from **Figure 7B**, nodes 4–18 all have voltage overrun risks according to the risk indicators proposed in this study, that is, most nodes have voltage crossing probability. It can be seen that as the deterministic assessment ignores the "probability" and uncertainty, the assessment results do not reflect the actual operating conditions.

As there are differences in the short-term safety risk of DG and EV access to the AC–DC distribution network at different time sequences, the results of the AC node voltage crossing risk indicators at each time are obtained on the basis of **Figure 7**, taking into account the time sequence, as shown in **Figure 8**. This is due to the fact that nodes 18 and 33 are at the end of the distribution system and have a short electrical distance from the DG or EV. The temporal variation also has a significant impact on the power quality of nodes 5–18 and 25–33. The temporal dimension shows that the AC distribution network nodes experience voltage overruns between 06:00 and 19:00 when the EV charging load is small and the DG output is too high; in addition, a large number of taxis charge quickly between 01:00 and 05:00, resulting in a certain voltage overrun at the nodes. In addition, a large number of taxis charge quickly between 01:00 and 05:00, resulting in a certain voltage overrun at the node. The DC distribution network node voltage is constant, and there is no node voltage overrun, which indicates that the DC distribution network node is not affected by the time series change and is relatively stable **Table 1** shows the risk index results of line power overrun. It can be seen from the table that during the period of 20:00–21:00, the risk of line power over-limit is mainly concentrated at the head end of the distribution network. Line 1–2 has the greatest risk of line power over-limit. This period is also the superposition of EV charging load and conventional load. The peak value of the power line leads to the greatest risk of line power violation.

Economic Risk Indicator Analysis

Figure 9 gives the results of the AC and DC line power overrun risk indicators. From **Figure 9A**, it can be seen that in the 20:00–21:00 time period, line power overrun risk is mainly concentrated at the head of the AC distribution network. From **Figure 9B**, it can be found that at 21:00, line 1–2 has the highest risk of line power overrun, which is also the peak of EV charging load and conventional load superposition, resulting in the highest risk of line power overrun. As can be seen in **Figures 9C,D**, branch tide

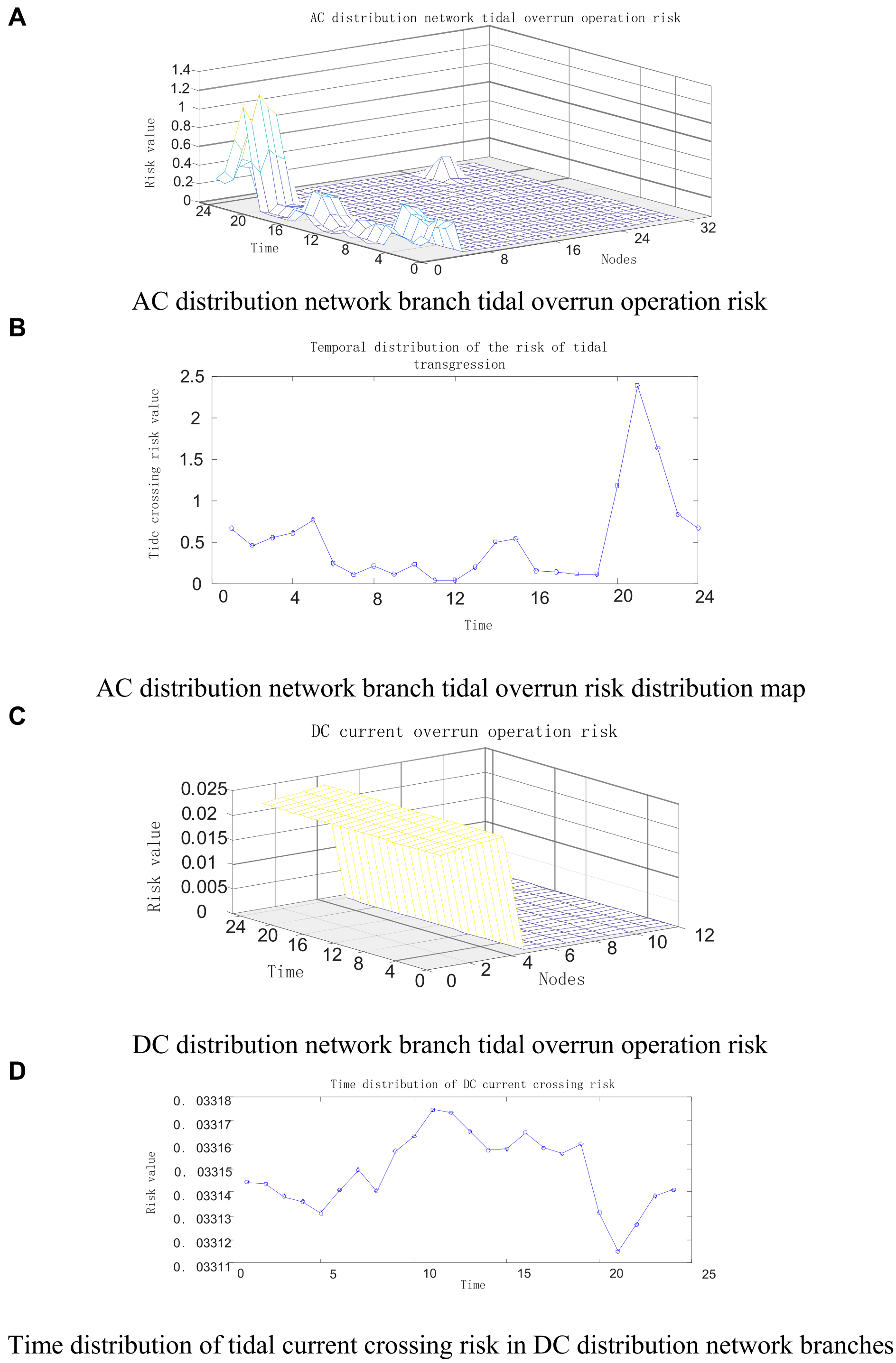

FIGURE 9 | AC and DC distribution network branch current overrun operational risk: **(A)** AC distribution network branch tidal overrun operation risk. **(B)** AC distribution network branch tidal overrun risk distribution map. **(C)** DC distribution network branch tidal overrun operation risk. **(D)** Time distribution of tidal current crossing risk in DC distribution network branches.

overruns occur in the DC distribution network during the 06:00–19:00 time period, and the risk values are greater than those in other time periods due to the smaller EV charging load and excessive DG output power in the AC distribution network at this time.

Analysis of Economic Risk Indicators

After the time-series economic risk assessment, the ERI results of AC and DC distribution networks for one day can be obtained as shown in **Figure 10**. From **Figure 10A**, it can be seen that the C_{ERI} is positive

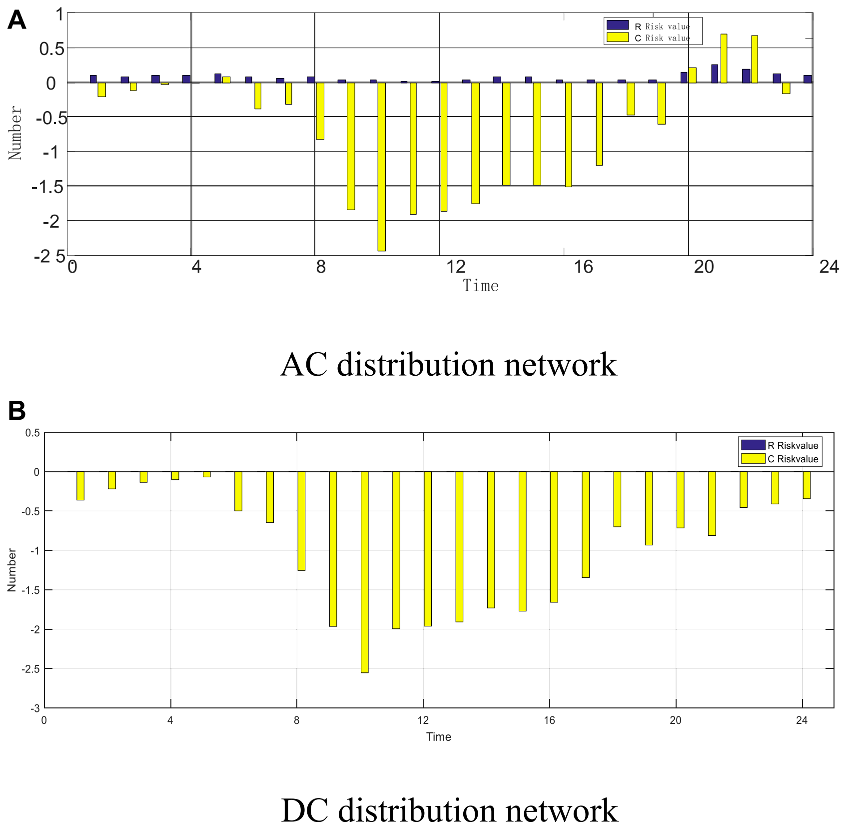

FIGURE 10 | ERI results of the distribution network: **(A)** AC distribution network. **(B)** DC distribution network.

during the 05:00 and 20:00–22:00 time periods, with the maximum value occurring during the 21:00–22:00 time period. The most risky time period is 20:00–22:00 when the risk values for both economy and safety are high due to the superposition of the conventional load and the EV charging load reaching peak load. At the same time, the operational state of the distribution network can be divided into the following two categories: ①During the periods 06:00–19:00 and 23:00–03:00, the value of the R_{SRI} is greater than 0, while the value of C_{ERI} is less than 0. This indicates that the operational state is economic but unsafe, and measures should be taken to reduce the R_{SRI}, for example, by reducing the output power of the DG and increasing the charging power of the EV station. ② The values of R_{SRI} and C_{ERI} are both positive during the hours of 04:00–05:00 and 20:00–22:00, indicating that the operating state of the distribution network is neither safe nor economical at this time due to the huge load demand and the fluctuation of DG output, and measures should be taken to improve the operating quality of the actual distribution network. As can be seen in **Figure 10B**, the value of R_{SRI} is almost zero and the value of C_{ERI} is less than zero at all times in the DC distribution network, which is both safe and economical.

Comprehensive Operation Risk Analysis Of DG And EV Connected To Distribution Network

From the previous simulation results, it can be seen that the short-term safety risk index and economic risk index at 21:00 reach the maximum value. Therefore, the risk value at 21:00 is selected, and the EV capacity is increased from 9 to 15 MW at intervals of 0.5 MW; 13 EV capacity values. According to the definition of risk indicators in **Section 3**, a 4 × 13-order risk indicator matrix is constructed. The risk index matrix was processed by the Z-Score method, and the standardized risk index results under each EV capacity were obtained. The KMO (Kaiser–Meyer–Olkin) test obtained by SPSS software simulation is 0.770, and the significance is less than 0.05. The results show that there is a strong correlation between the risk indicators, and factor analysis can be carried out.

The factor analysis in PCA is used to reduce the dimension of the risk index matrix, and the related factor loading matrix of the risk index and y_1 is obtained. It can be seen from the table that all risk indicators have a high correlation with the first principal component, that is, y_1 reflects 98.3% of ELLR information, 97.7% of EPLR information, 97.7% of line power over-limit risk information, and 98.8% of the node voltage violation risk information. According to formula **Eq. 25**, the cumulative contribution rate γ = 96.279% is calculated, so y_1 can represent the original four risk indicators to achieve the purpose of reducing the dimension of the original risk indicators.

According to formula **Eq. 24**, the scores of each risk index can be calculated, and the results are shown in **Table 6**. It can be seen from **Table 6** that the importance

TABLE 6 | Component score coefficient.

Index	Node voltage over-limit risk	Line power limit risk	ELLR	EPLR
Score	0.256	0.254	0.256	0.253

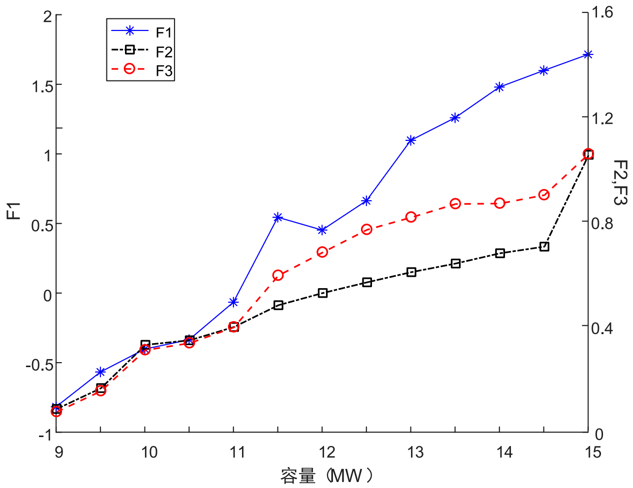

FIGURE 11 | Comprehensive risk assessment indicator results with different EV capacities.

of each risk index is related, and the node voltage over-limit risk index has the largest weight, which is also an important basis for the next stage of the distribution network to be transformed.

In order to better reflect the superiority of the method in this study, it is compared with the comprehensive risk assessment method based on weighted entropy in literature (Yang et al., 2020b) and the traditional voltage and power flow out-of-limit comprehensive risk evaluation method in literature (Hou, 2017). When DG and EV are connected to the distribution network at the same time, the comprehensive risk assessment index results under different EV capacities are shown in **Figure 11**. In the figure F_1, F_2, F_3 are the comprehensive risk assessment index results of the method in this study, the method implemented by Yang et al., (2020b), and the method implemented by Hou, (2017), respectively.

It can be seen from **Figure 11** that with the continuous increase of EV capacity, the comprehensive risk value only considering safety factors continues to increase. However, using the method in this study, it can be found that when the EV capacity is within the 12 MW range, the comprehensive risk assessment index value of the distribution network decreases, which has a mitigating effect on the operation of the distribution network. It can be seen that it is better to consider the risk factors such as safety and economy at the same time. It can accurately grasp the operation risk status of the distribution network and can play a positive role in guiding EV access to the distribution network capacity.

CONCLUSION

In this study, a risk analysis method for grid-connected operation of EVs in AC–DC distribution networks is proposed, and the conclusions obtained are as follows.

1) In considering the impact of DG and EV on the AC–DC distribution network, a CC–CV variable power charging load model without subjective prediction laws is established, which avoids the shortcomings of the commonly used EV charging load modeling methods, such as the incompatibility between the model with artificially set parameters and the random driving characteristics of users, and can reflect the actual charging characteristics of EV more realistically.
2) Compared with deterministic assessment, the short-term safety risk index based on the complex network theory proposed in this study can more realistically reflect the short-term safety risk caused by the uncertainty of the distribution network node; the greater the security risk is.
3) Using the ERI with ELLR and EPLR, it is verified through simulation that the distribution network has economic risk during the hours of 04:00–05:00 and 20:00–24:00, and the distribution network can obtain certain economic benefits during other hours.
4) Based on the proposed risk index, the risk index matrix of different EV capacities connected to the distribution network is constructed, and PCA is used to conduct comprehensive risk assessment. The results show that with the increase of EV capacity, the comprehensive risk assessment index value also increases, but the comprehensive risk has been alleviated within a certain range, and EV charging can be better guided. In addition, the weight coefficient of the risk index is calculated by PCA, which effectively avoids the deviation caused by the adverse influence of other subjective factors.

DATA AVAILABILITY STATEMENT

The raw data supporting the conclusions of this article will be made available by the authors, without undue reservation.

AUTHOR CONTRIBUTIONS

JD, JZ, and YL made important contributions to the concept, idea, topic selection, design and data acquisition, analysis, or interpretation of the research work; ZL and ZY wrote the manuscripts or modified their key contents; JL and ZW comprehensively reviewed and checked the final published articles.

FUNDING

This research was funded by Science and Technology Project of State Grid Jibei Electric Power Co., Ltd. (2021 research on distribution flexible DC networking technology of State Grid Jibei intelligent distribution center B30144210005).

REFERENCES

Chen, L., Zhang, Y., and Figueiredo, A. (2019). Overview of Charging and Discharging Load Forecasting for Electric Vehicles[J]. *Automation Electric Power Syst.* 43 (10), 269–289. doi:10.7500/AEPS20180814001

Guo, C., Liu, D., and Zhu, C. (2020). Modeling and Analysis of Electric Vehicle Charging Load in Residential Area[J]. *Electric Power Automation Equipment* 40 (1), 1–9. doi:10.16081/j.epae.201912015

Hou, Y. (2017). *Risk and Safety Assessment of Distribution Network with Distributed Generation and Electric vehicle[D]*. Changsha: Hunan University.

Hu, W., Wu, W., and Wanmeng, H. (2016). Operation Risk Assessment on Distribution System with the Integration of Electric Vehicles[J]. *Mod. Electric Power* 33 (2), 45–50. doi:10.19725/j.cnki.1007-2322.2016.02.008

Ju, L., Tan, Q., Lu, Y., and Tan, Z. (2019). A CVaR-Robust-Based Multi-Objective Optimization Model and Three-Stage Solution Algorithm for a Virtual Power Plant Considering Uncertainties and Carbon Emission Allowances[J]. *Int. J. Electr. Power Energ. Syst.* 107 (MAY), 628–643. doi:10.1016/j.ijepes.2018.12.012

Li, H., Lu, Z., and Qiao, Y. (2015). Assessment on Operational Flexibility of Power Grid with Grid-Connected Largescale Wind Farms[J]. *Power Syst. Technology* 39 (6), 1672–1678. doi:10.13335/j.1000-3673.pst.2015.06.032

Li, Y., Han, M., Yang, Z., and Li, G. (2021). Coordinating Flexible Demand Response and Renewable Uncertainties for Scheduling of Community Integrated Energy Systems with an Electric Vehicle Charging Station: A Bi-level Approach. *IEEE Trans. Sustainable Energ.* 12 (4), 2321–2331. doi:10.1109/tste.2021.3090463

Liang, Y., Wu, Y., and Zhao, M. (2020). Technical Analysis and Development prospect of New Generation Low-Voltage DC Power Supply System in the "new Infrastructure" [J/OL]. *Chin. J. Electr. Eng.* 1-13–1128. doi:10.13334/j.0258-8013.pcsee.201180

Liu, P., Li, H., Zhao, Y., and Zeng, K. (2015). Power Grid Security Risk Assessment Considering Comprehensive Element Importance Index[J]. *Electric Power Automation Equipment* 35 (4), 132–138. 144. doi:10.16081/j.issn.1006-6047.2015.04.020

Liu, S., Zhao, B., and Wang, X. (2017). Capacity Configuration Model for Robust Optimization of Stand-Alone Microgrid Based on Benders Decomposition[J]. *Automation Electric Power Syst.* 41 (21), 119–126.

Lu, D., and Yuan, Y. (2017). Weak Part Identification Based Onfault-Tree Monte Carlo Simulation for Islanded Microgrid[J]. *Electric Power Automation Equipment* 37 (4), 38–44. doi:10.16081/j.issn.1006-6047.2017.04.006

Nan, Q., Mu, Y., and Dong, X. (2020). Comprehensive Evaluation index System and Method for Fast Charging Network of Electric Vehicles[J]. *Automation Electric Power Syst.* 44 (1), 83–91. doi:10.7500/AEPS20190408004

Shi, W., Li, X., and Wang, X. (2018). Vul-nerability Assessment Method for Distribution Network[J]. *Proc. CSU-EPSA* 30 (12), 125–131. doi:10.3969/j.issn.1003-8930.2018.12.019

U.S. Department of Transportation (2018). "Federal Highway Administration," in *National Household Travel survey[EB/OL]*. [2019-03-20]Avialable at: http://nhts.ornl.gov.

Wang, L., Liu, C., and W, B. (2018). Risk Based Assessment Method for Transmission System Considering the Influence of Micro-grid Charging Station[J]. *Power Syst. Prot. Control.* 46 (5), 114–121. doi:10.7667/PSPC170232

Xiao, B., Liu, Y., and Shi, Y. (2018). Power Supply Reliability Assessment of Mid-voltage Distribution Network Based on Principal Component Analysis[J]. *Electric Power Automation Equipment* 38 (10), 7–12. doi:10.16081/j.issn.1006-6047.2018.10.002

Xiong, F., Dong, B., and Li, G. (2016). Risk Evaluateon of Distribution System with Stochastic Distributed Generator[J]. *Automation Electric Power Syst.* 40 (12), 62–67. doi:10.7500/AEPS20160118007

Yang, J., Yi, Y., and Zhang, Y. (2020b). Operation Risk Analysis of Electric Vehicle Integrated to Distribution Network Based on Weighted Distribution Entropy [J]. *Automation Electric Power Syst.* 44 (5), 171–179. doi:10.7500/AEPS20190303007

Yang, M., Dai, B., and Liu, L. (2020a). A Review of Wind Power Probabilistic Prediction[J]. *J. Northeast Electric Power Univ.* 40 (02), 1–6. doi:10.19718/j.issn.1005-2992.2020-02-0001-06

Yuan, J., Wang, X., and Shen, G. (2016). Static Security Analysis of Power Grid Based on Comprehensive Risk Index[J]. *Proc. CSU-EPSA* 28 (10), 129–134. doi:10.3969/j.issn.1003-8930.2016.10.022

Zhang, J., Zhang, P., Wu, H., Qi, X., Yang, S., and Li, Z. (2019). Reliability and Risk Analysis of Load Aggregators in Demand Response [J]. *Acta Energiae Solaris Sinica* 40 (12), 3526–3533.

Zhang, S., Cheng, H., Zhang, L., Masoud, B., and Liangzhong, Y. (2013). Probabilistic Evaluation of Available Load Supply Capability for Distribution System[J]. *IEEE Trans. Power Syst.* 28 (3), 3215–3225. doi:10.1109/tpwrs.2013.2245924

Zhao, W., Jiang, F., and Tu, C. (2014). Harmonic Currents of Grid-Connected EV Charging Station[J]. *Electric Power Automation Equipment* 34 (11), 61–66. doi:10.3969/j.issn.1006-6047.2014.11.010

Zhao, Y., Zhou, J., and Liu, Z. (2009). Convergence Analysis and Comparison of Sequential and Nonsequential Monte-Carlo Simulation for Bulk Power System Reliability Assessment[J]. *Trans. China Electrotechnical Soc.* 24 (11), 127–133. doi:10.3321/j.issn:1000-6753.2009.11.020

Zheng, J., Dai, M., Zhang, M., and Wang, W. (2012). Load Cluster Characteristic and Modeling of EV Charge Station in Residential District[J]. *Proc. CSEE* 32 (22), 32–38. doi:10.13334/j.0258-8013.pcsee.2012.22.009

Conflict of Interest: JD, JZ, YL, and JL were employed by Smart Distribution Network Center, State Grid Jibei Electric Power Co. Ltd. This study received funding from Science and Technology Project of State Grid Jibei Electric Power Co., Ltd. The funder had the following involvement with the study Electric vehicle modelling.

The remaining authors declare that the research was conducted in the absence of any commercial or financial relationships that could be construed as a potential conflict of interest.